X-ray irradiation of soda-lime glasses studied *in situ* with surface plasmon resonance spectroscopy

A. Serrano,[1,a)] F. Gálvez,[2] O. Rodríguez de la Fuente,[2] and M. A. García[1,3]
[1]*Instituto de Cerámica y Vidrio (ICV-CSIC), Cantoblanco, 28049 Madrid, Spain*
[2]*Departamento de Física de Materiales, Universidad Complutense de Madrid, 28040 Madrid, Spain*
[3]*IMDEA Nanociencia, Cantoblanco, 28049 Madrid, Spain*

(Received 10 October 2012; accepted 22 February 2013; published online 18 March 2013)

We present here a study of hard X-ray irradiation of soda-lime glasses performed *in situ* and in real time. For this purpose, we have used a Au thin film grown on glass and studied the excitation of its surface plasmon resonance (SPR) while irradiating the sample with X-rays, using a recently developed experimental setup at a synchrotron beamline [Serrano *et al.*, Rev. Sci. Instrum. **83**, 083101 (2012)]. The extreme sensitivity of the SPR to the features of the glass substrate allows probing the modifications caused by the X-rays. Irradiation induces color centers in the soda-lime glass, modifying its refractive index. Comparison of the experimental results with simulated data shows that both, the real and the imaginary parts of the refractive index of soda-lime glasses, change upon irradiation in time intervals of a few minutes. After X-ray irradiation, the effects are partially reversible. The defects responsible for these modifications are identified as non-bridging oxygen hole centers, which fade by recombination with electrons after irradiation. The kinetics of the defect formation and fading process are also studied in real time. © *2013 American Institute of Physics*. [http://dx.doi.org/10.1063/1.4794807]

INTRODUCTION

Glassy materials present very appealing optical and electrical properties for various industrial applications including optical fibers, optical components, hot-cell windows, or reactors. Their advantages mainly relay on low cost and high optical transparency, which extends from the infrared to ultraviolet regions.[2–5] High energy ionizing radiation (X-rays, gamma rays, electrons, etc.) can induce numerous changes in glasses, being the visible coloration one of the most obvious.[2,6–8] In particular, X-ray irradiation induces color centers in glasses,[9,10] prompting a great interest since the defects can be generated and bleached reversibly.[11] Most glassy materials present a structure with modifier ions or dopants that are incorporated into the glass network. The radiation induced color centers are typically associated with those modifiers, leading to the formation of these defects responsible for the glass darkening.[12] These centers can alter some physical properties of the glasses such as the optical absorption,[9,11] refractive index,[13] axial stress[14] or thermal expansion coefficient.[6]

It is often necessary that the glassy materials properly respond under radiation[2,5] for a specific application. Therefore, studies on defects in glasses induced by X-ray irradiation are important to determine their nature, the possible mechanisms during and after the radiation and the changes on the glass properties. In the literature, some works have studied the formation and fading dynamic of color centers and their possible effects on physical properties when these defects are induced.[2,6,7] Most of these studies devoted to analyze the effect of X-ray irradiation onto soda-lime glasses are carried out by irradiating the sample and analyzing later their optical properties.[9–12] However, studies in real time and *in situ* are necessary for a deeper understanding of the process. Otherwise, processes associated with fast dynamics can be missed. Hence, the chance of measuring *in situ* optical properties of glasses while they are being irradiated is an appealing possibility. Performing ellipsometric measurements in combination with X-ray irradiation is complicated. Optical absorption spectroscopy can be easier to combine with X-ray irradiation but it just rends information about the imaginary part of the refractive index. However, surface plasmon resonance (SPR) spectroscopy provides, simultaneously, information on the modification of the real and imaginary parts of the refraction index.

We have recently developed a set-up for the measurement of SPR of metallic films at a synchrotron beamline.[1] The device follows the Kretschmann-Raether configuration and allows the simultaneous measurement of SPR and X-ray absorption spectroscopy (XAS). Hence, it permits the measurement of SPR *in situ* while the system is being irradiated. SPR in metallic films is very sensitive to the features of the surrounding media, and thus, to the substrate.[15] Measuring SPR curves of metallic films grown on soda-lime glasses while irradiating with X-rays allows tracking changes in the real and imaginary parts of the refractive index of the glass in real time.

In this work, we have prepared Au thin metallic films onto soda-lime glasses and used the above mentioned device to study *in situ* the effect of X-ray irradiation on the glass. In particular, we have studied the dynamics of formation and decay of color centers in real time.

EXPERIMENTAL

We used commercial soda-lime glass substrates composed of SiO_2 73%, Na_2O 14%, CaO 7%, MgO 4% and

[a)]Author to whom correspondence should be addressed. Electronic mail: aida.serrano@icv.csic.es.

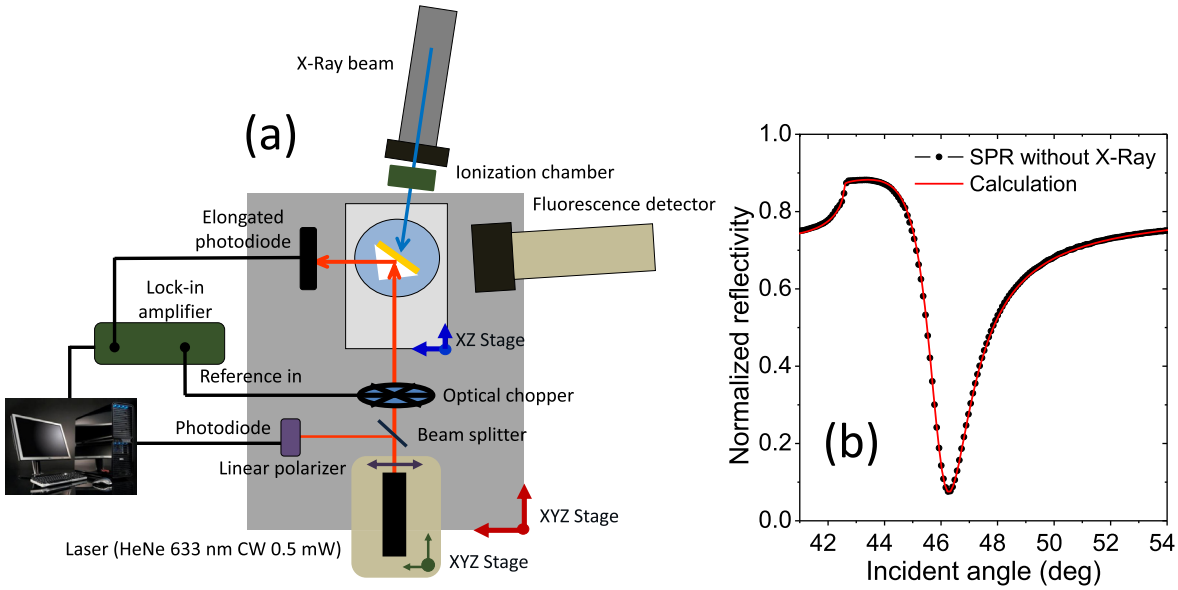

FIG. 1. (a) Scheme of the device for simultaneous SPR and XAS measurements. (b) Experimental (black solid circles) and calculated (red solid line) SPR curve of a 42 nm Au film on soda-lime substrate without X-ray irradiation.

Al_2O_3 2%, with a thickness of 1 mm and a refractive index n = 1.513 ($\lambda = 645$ nm). Soda-lime substrates were cleaned with soap and water, and dried with dry air flux. Au thin films (42 nm) were deposited on the soda-lime substrates by thermal evaporation using a home-made evaporation chamber. Au wire (99.99% purity, 0.5 mm diameter) was placed onto a tungsten "V"-shape filament and was initially melted to form a ball. Substrates were placed 15 cm away from the filament and the deposition was performed under a 10^{-6} Torr pressure with currents of 26 A at a rate of 0.02 nm s^{-1}, controlled with a Q-microbalance.

Experiments were carried out at the branch A of the BM25 SpLine beamline at the European Synchrotron Radiation Facility (ESRF) in Grenoble (France). This is a hard X-ray beamline arranged to perform XAS. The energy range of X-rays is between 5 and 45 keV and the flux is of the order of 10^{12} photons/s at 200 mA ring current.[16] In the experimental hutch, we have mounted the SPR device previously described.[1] Figure 1(a) shows a scheme of the system which follows the Kretschmann-Rather configuration.[15] Briefly, the sample is attached to a quartz prism (n = 1.457 at $\lambda = 633$ nm) through the glass side using gel index matching. The sample is illuminated with a laser through the prism in total reflection conditions. The evanescent field propagates across the Au film reaching the Au/air interface. For the proper incidence angle, the dispersion relation of the evanescent film matches that of the surface plasmons that are excited at the Au/air interface. The electromagnetic field propagates through the Au film towards the glass and interferes destructively with the incidence laser beam, reducing the intensity of the reflected beam. Recording the intensity of the reflected beam as a function of the incidence angle yields the SPR curve as that shown in Figure 1(b). In our experimental results, the incident angle corresponds to the original angle of the laser beam with respect to the film surface (before being refracted at the prism surface), also called external angle. The device allows detecting a relative variation in the curve of the order of 10^{-3}–10^{-4}.[1] The proper performance of the device was tested comparing the SPR spectrum measured for a 42 nm Au film grown onto soda-lime glass with a simulated spectrum, as shown also in Figure 1(b).

For the measurement of SPR upon X-ray irradiation, the samples were simultaneously illuminated with the laser from the prism side and the X-rays from the Au film side, making the spots coincident at the Au film side. Although the X-ray beam reaches the Au film, the skin depth for hard X-rays in Au is of the order of several microns, so X-rays pass through the 42 nm Au film reaching the substrate at the same position that the laser spot.

Samples were irradiated with X-rays around the Au L3 edge at different energies: 11.80 keV, 11.92 keV and 11.95 keV, which correspond to energies below, at and above the absorption edge, respectively. Much weaker effects were also observed at lower energies (6 to 8 keV).

Simulations of SPR spectra were performed with WINSPALL, a freeware software to simulate SPR spectra with great accuracy.[17] This code is based on the Fresnel equations for the system, including the correction of both reflection and refraction of the coupling prism.

Optical absorption spectra of the glasses were recorded using a V-670 UV-visible double beam spectrophotometer in transmission mode at room temperature ranging between 280 and 800 nm.

RESULTS AND DISCUSSION

Figure 2(a) shows experimental SPR spectra for a 42 nm Au film grown onto a soda-lime substrate glass before, during and after X-ray irradiation at 11.92 keV. Irradiation induces a decrease in the intensity of the reflected beam for the whole SPR curve. This behavior is due to the darkening

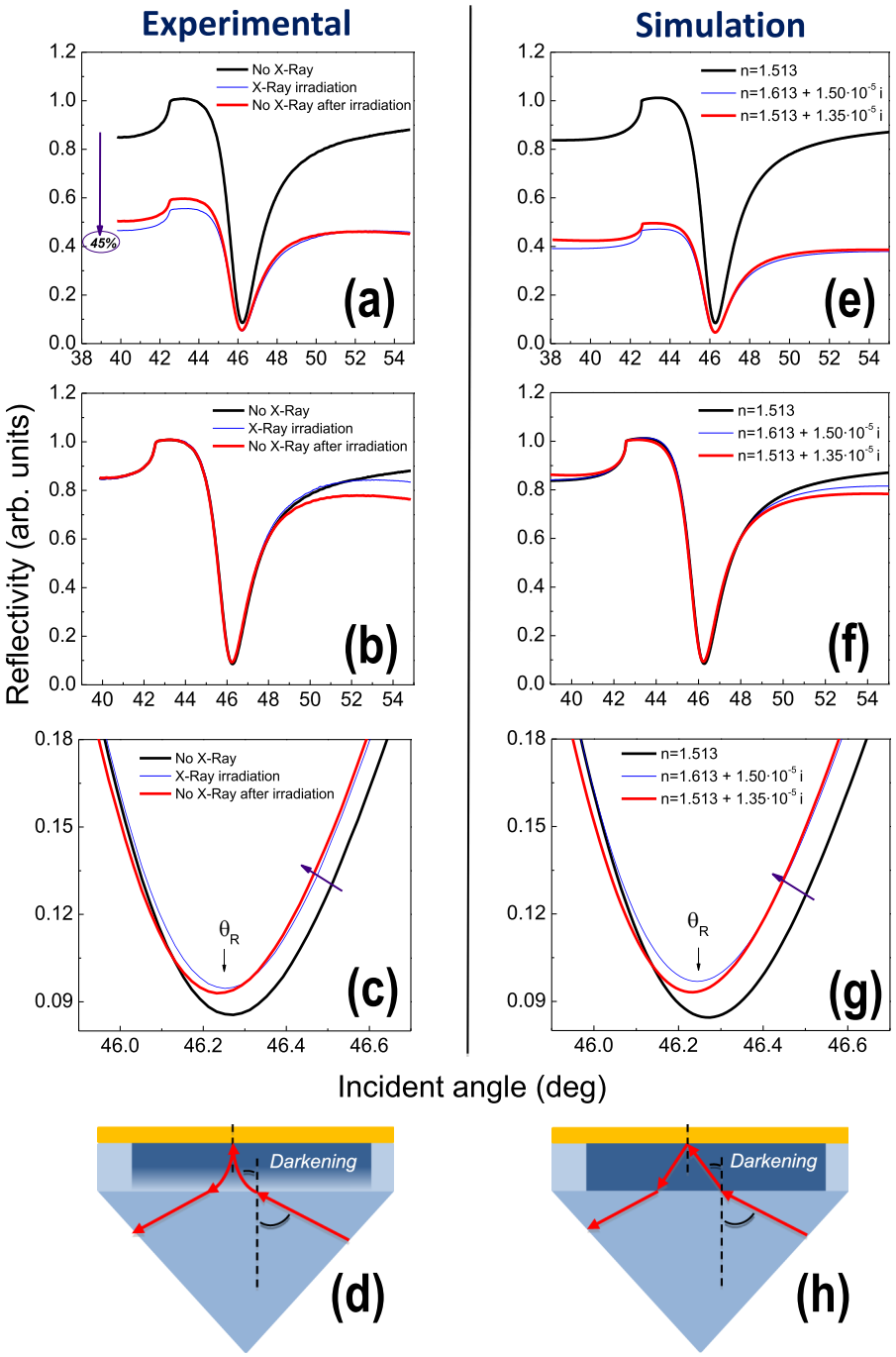

FIG. 2. (a)-(c) SPR curves for a Au film on soda-lime glass before (black line), during (blue line), and after (red line) irradiation with 11.92 keV X-rays. (a) Spectra as measured, (b) spectra normalized at the critical angle and (c) a detail of the resonance region for the normalized spectra. (e)–(g) Calculated SPR spectra using the parameters indicated in the legend. (e) Unnormalized spectra, (f) spectra normalized at the critical angle, (g) a detail of the resonance region for the normalized spectra. (d) and (h) Scheme of the four-media system (darkening is decreasing inside the soda-lime glass) and the model used for the simulations (darkening is homogeneous), respectively.

of the glass upon X-ray irradiation, which was observable with the naked eye. When measuring SPR, the laser beam propagates through the glass substrate and it is partially absorbed reducing its intensity. The effect is accumulative: the larger the irradiation time, the larger the decrease of the intensity. In particular, SPR spectrum intensity decreases about 45% after 230 min of X-ray irradiation. When switching off the X-rays, the reflected intensity of SPR spectrum increases, pointing out that the irradiation effects are partially reversible: after 170 min without X-ray irradiation, the SPR spectrum intensity increases from 45% to 49% of the value of the initial spectrum. SPR spectra of Au films onto pure silica glasses did not show this phenomenology upon irradiation. Thus, the variations in intensity observed here correspond entirely to changes in the soda-lime glass and we may discard as they are due to modifications in the Au film. The glass darkening is due to the formation of color centers upon irradiation. These defects are unstable at room temperature, so the darkening is partially reduced with time after irradiation. However, the initial reflectivity values are not completely recovered with time (months are necessary).[9] Figure 2(b) shows the normalized reflected intensity of the SPR spectra measured before, during and after irradiation. It can be observed that the shape of SPR curve changes at larger incident angles when the sample was irradiated. This effect was not recuperated when the X-rays were switched off but it was even deeper.

In the SPR spectra, we can analyze the resonance angle which is extremely sensitive to any change in the refractive index of the glass substrate. This corresponds to the incident angle for which the reflected intensity shows a minimum.[15] Upon irradiation, the resonance angle slightly shifts towards

lower angles and the bandwidth is somehow reduced. These effects increase with irradiation time. For 230 min irradiation, the shift was about 0.04° (Figure 2(c)). Neither the shift nor the narrowing of the resonance is reversible after irradiation.

The critical angle does not change upon X-ray irradiation, but it depends just on the refractive index of the quartz prism and the air (see Figure 2). The total refraction takes place at the soda-lime/Au interface. When the laser passes from the prism to the soda-lime glass, according to Snell laws, the refraction keeps the component of the light wavevector parallel to the surface in both media constant. Since the critical angle is determined by this component, it will not depend on the particular value of the refractive index of the soda-lime glass.

It is well known that the refractive index in glasses increases by exposing them to X-ray radiation[13] or UV laser pulses.[18] The glass presents, in our case, a profile density of the induced defects which is maximum at the Au/glass interface and decreases exponentially inside the glass (see Figure 2(d)). It can be observed that the darkening comes across the whole glass, being even transmitted (but with low intensity) into the prism. However, simulations of the SPR spectra result are too complicated if this gradient is fully taken into account. Instead, we have considered a homogeneous darkening along the whole soda-lime substrate, which has a thickness of 1 mm (see Figure 2(h)). This approach has allowed us to study semi-quantitatively the modifications of the glass induced by the X-rays in the optical properties of the glass. Therefore, the obtained values for the refractive index are approximated and show a tendency rather than exact values.

We have performed the SPR simulations varying the refractive index of the modified layer, in our four-media system, in order to reproduce the experimental results presented in Figures 2(a)–2(c). In these simulations, we have considered two glass media: an infinite one described with the parameters of the unmodified quartz prism (i.e., $n_{glass} = 1.457$) plus a 1 mm layer (soda-lime glass) with modified properties that are indicated in the legend of the figure. The refractive index of soda-lime glass upon X-ray irradiation is determined by fitting the experimental SPR curve. In this fit, the refractive index of the soda-lime glass is the only free parameter, while the rest of parameters remain fixed with the same value as those prior to X-ray irradiation. Figures 2(e)–2(g) show the results of the fits. We can obtain a very good agreement with the experimental results assuming that the refractive index of the modified layer upon irradiation changes from $n_{glass} = 1.513$ (non-irradiated value) to $n_{glass} = 1.613 + 1.50 \times 10^{-5}$ i (see Figures 2(d)–2(f)). To reproduce the fine changes in the structure of the resonance, we need to consider also a slight modification in the Au effective refractive index of the order of 1%. A modification of the Au intrinsic refractive index induced by the X-ray irradiation is not likely. The modification might be rather due to structural or electric modifications in the glass/Au interface upon irradiation. It can be also due to the adsorption, induced by irradiation, of molecular or atomic species or impurities at the surface of Au, such as atomic oxygen, when the surface is eventually exposed to the ozone[19] produced by synchrotron radiation. Note that, with the reported values, we reproduce simultaneously the reduction in the intensity, the change of the spectrum profile at large incident angles, the shift of the resonance angle towards smaller values and the decrease of the bandwidth (compare experimental results with simulations in Figure 2). Regarding the partial recovery of the SPR signal after irradiation, we may reproduce the observed behavior assuming that the modification of the real refractive index is totally recovered, while the modification of imaginary one is almost permanent (recovery of only 10% after 170 min).

As mentioned above, glass darkening upon X-ray irradiation is due to the generation of color centers.[9] These color centers are attributed to the formation of electron-hole pairs which, in turn, can yield the creation of defects, causing high absorbance in the UV and visible region. According to the literature,[2,20,21] radiation induces defects on glasses associated with either oxygen excess or oxygen defect in the network. For soda-lime glass, the most typically reported defects are non-bridging oxygen hole centers (NBOHCs: ≡Si-O*), E′ centers (≡Si*), peroxy radicals (PORs:≡Si-O-O*), and trapped electrons (TEs), where the symbol "≡" denotes three bonds with other oxygen in the glass network and the "*" represents an unpaired electron.[2,20]

A proper identification of the type of color center can be obtained by optical absorption spectroscopy, since each of these defects induces absorption bands at different wavelengths.[9,10] Figure 3 shows the optical absorption spectrum of an irradiated soda-lime glass (referenced to non-irradiated soda-lime glass in order to obtain the net irradiation induced absorption) measured 1 month after the irradiation. The spectrum can be decomposed into three gaussian bands (with a coefficient of determination $R^2 = 0.99977$). In this way, the

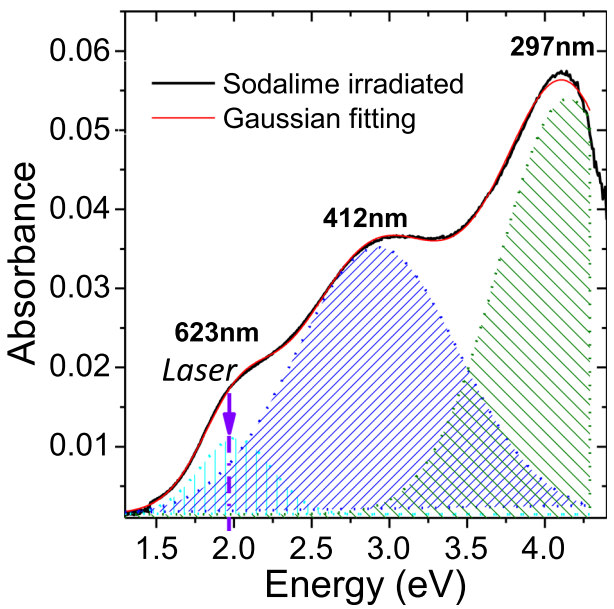

FIG. 3. Optical absorption spectrum for a soda-lime glass irradiated at E = 11.80 keV (black line) and the fit (red line) to three gaussian bands associated with the induced absorptions. The measurement was performed 1 month after X-ray irradiation. The bands at 623 nm and 412 nm correspond to NBOHCs defects and the band at 297 nm corresponds to TE defects.

TABLE I. Parameters corresponding to the three gaussian fit of the optical absorption bands for soda-lime glass irradiated with X-rays at E = 11.80 keV.

Wavelength (nm)	Energy (eV)	Width (eV)	Defect
623.3 ± 0.2	1.990 ± 0.001	0.385 ± 0.002	*HC*1
411.7 ± 0.3	3.012 ± 0.002	1.347 ± 0.002	*HC*2
297.3 ± 0.1	4.171 ± 0.001	0.765 ± 0.002	*TE*

three characteristic absorption bands with maxima at 623 nm, 412 nm, and 297 nm (2.0 eV, 3.0 eV, and 4.2 eV, respectively) were resolved. Table I summarizes the main features of these absorption bands.

According to the literature, the bands at 623 nm and 412 nm are associated with the induced defects of NBOHCs,[2,20] being responsible for the brown color, while the band of 297 nm was identified as absorption of TE.[9]

There are two types of NBOHC defects, designed as HC1 and HC2, which are paramagnetic and dominate the optical absorption spectra of glasses with low and high alkali contents, respectively.[22] The band at 623 nm (HC1) corresponds to a hole trapped in the 2p orbital of one non-bridging oxygen at those sites of the network where the SiO_4 polyhedron contains three bridging oxygen and one non-bridging oxygen, all bonded to a silicon atom. HC2 defects are responsible for the absorption band around 412 nm, which is associated with a hole trapped in two or three non-bridging oxygen bonded to the same silicon.[11,23,24] In our SPR experiments, we are using a 633 nm laser, and thus the observed absorption at this wavelength is due to both HC1 and HC2 defects (see Figure 3).

The formation of NBOHC defects in a glass upon X-ray irradiation starts with the formation of electron-hole pairs. In silica based glasses, the holes are trapped by the non-bridging oxygen atoms yielding the formation of NBOHCs, while electrons diffuse through the glass network. Since these defects are unstable at room temperature, they can be eliminated after irradiation by recombination with electrons or other NBOHCs according to the following reactions:[2,9]

$$\equiv Si - O^* + e^- \rightarrow Si - O^-, \quad (1)$$

$$2(\equiv Si - O^*) \rightarrow Si - O - O - Si \equiv, \quad (2)$$

$$2(\equiv Si - O^*) \rightarrow Si - O - Si \equiv +{}^1/_2 O_2. \quad (3)$$

Paramagnetic defects as NBOHCs decay obeying first-order or second-order kinetics.[9,25] In particular, when the decay is due to recombination with electrons (reaction 1), it follows a first-order kinetic. On the contrary, NBOHCs that recombine with each other (reactions 2 and 3) exhibit a second order kinetics. Previous studies on X-ray irradiated soda-lime glasses demonstrated that the fading of color centers after irradiation presents a first-order decay.[9,11,26,27] However, these studies have been performed *ex situ* and measured over long times (days and/or months). Hence, the study of the kinetics in the order of seconds and/or minutes is still missing.

Using the SPR device, we have measured the reflectivity for a fixed incident angle close to the resonance (45.6°) when switching on and off the X-ray irradiation. These measurements could, in principle, have been carried out without the Au thin film or in transmission mode using the same set-up. Figure 4 shows the effect of X-ray irradiation on soda-lime glass at three different energies, 11.80 keV, 11.92 keV, and 11.95 keV, which are below, at and above the L3 edge of Au, to discriminate if part of the effects are due to X-ray absorption by the Au film. The results confirm that the reflectivity decreases upon irradiation and partially recovers with time after irradiation. Moreover, we found the kinetics of the process to be dependent on the X-ray energy. In particular, the decay results slower when using X-rays well above the Au L3 edge. These differences in decay rate cannot be associated with the reduction of X-ray intensity when passing through the Au film. Only 1% of the photons are absorbed in the film. However, the X-ray absorption in the film creates photoelectrons that can be ejected towards the glass modifying the lifetime of the defects.

The fitting of these curves to a first order kinetics (i.e., an exponential function) or to a second order kinetics was not satisfactory. However, as Figure 5 illustrates, these data can be properly fitted to the sum of two exponentials, according to the following equation:

$$I = I_0 + a \times e^{-t/\gamma_1} + b \times e^{-t/\gamma_2}, \quad (4)$$

where γ_1 and γ_2 represent decay constants and I_0, a, and b are fitting parameters.

As result of the exponential fitting (Eq. (4)), we conclude that the formation and fading of defects correspond to two kinetics of first-order, where the first-order half-life time, τ_i $(\imath = 1, 2)$ can be calculated from

$$\tau_i = \ln 2 \times \gamma_i. \quad (5)$$

These fittings have been carried out for the three energies studied obtaining coefficients of determination better than

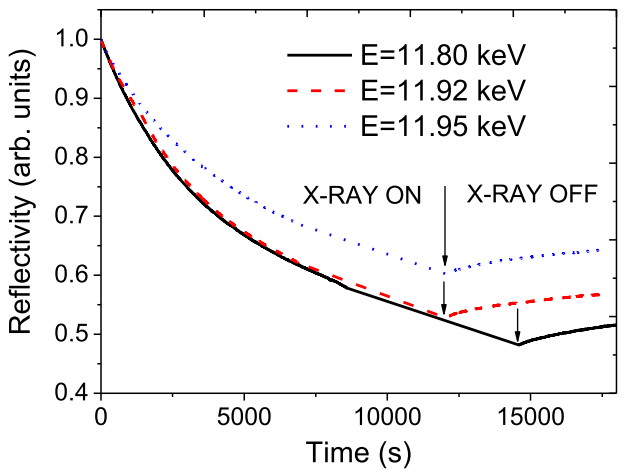

FIG. 4. Time dependence of the reflectivity when switching on and off the X-rays at three different energies (11.80 keV, 11.92 keV and 11.95 keV), *in situ* and in real time. The X-ray beam at 11.80 keV was switched off 2500 s later than the two other cases.

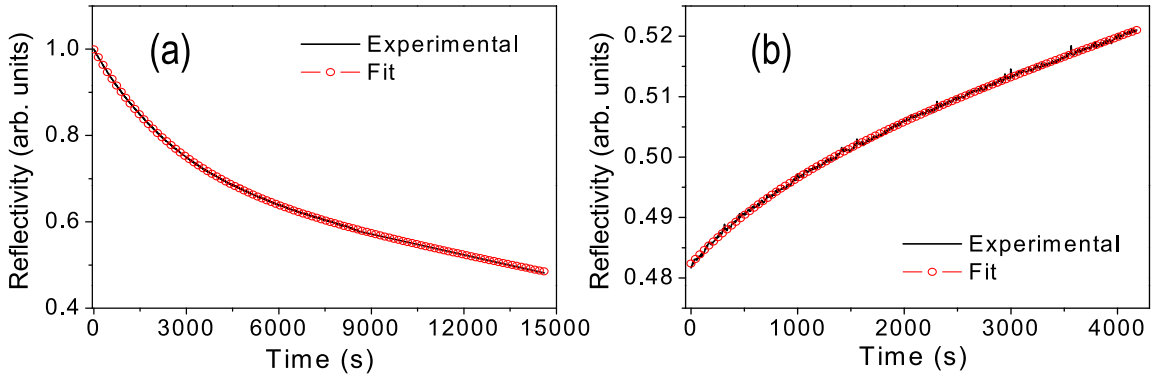

FIG. 5. Reflected intensity versus the time (solid black lines) and exponential fitting (red circles) of the color centers (a) formation and (b) fading by switching on and off X-rays at 11.80 keV, respectively, at an incident angle of 45.6°.

0.9987. Table II shows the parameters corresponding to the fittings for each energy. The decay of the color centers follows double first-order kinetics with decay times of the order of minutes and months. The latter is qualitatively in agreement with the previous studies *ex situ* of the irradiation effects.[9,10] On the contrary, the decay constant of the order of minutes has not been previously reported.

The fact that we have found just first-order kinetics in the fading curve points out that the NBOHC defects just recombine with the neighboring electrons (reaction 1) but not with another neighboring NBOHC or another holes (reactions 2 and 3).

The simulations of SPR spectra presented in Figure 2 show that the modifications in the real part of the refractive index are partially recovered in minutes after irradiation. On the other hand, the changes in the imaginary part of the refractive index remain almost unvaried for hours after irradiation. Thus, these changes in imaginary refractive index are mainly associated with the slow kinetics.

Regarding the nature of the two time components, a possible explanation could be that each of them is associated with one of the NBOHCs. However, in this case, the band associated with the fast kinetics should disappear from the spectrum after a few hours. Instead, we observe it clearly even after several days (see Figure 3). Moreover, Sheng *et al.*[9,10] found that the relative intensity of the bands associated with the NBOHCs does not change with time. Therefore, we conclude that the fading kinetics is governed by the availability of electrons to recombine with the NBOHCs (first-order kinetics). The existence of the two components rather supports that we have two types of electrons responsible for the fast and low kinetics. The electrons responsible for the fast component should be weakly trapped or nearly free so that they can move through the glass at room temperature, reaching the NBOHCs and recombining in minutes. On the other hand, the electrons associated with the slow kinetics should be those trapped in TE defects, well described in the literature.[2,9,20] The availability of these electrons for recombination is not determined by their mobility but by the probability to be released from a TE defect which at room temperature yields a decay time of months. As the fading kinetic for both NBOHCs is determined by the presence of electrons available for recombination, the decay rate is the same for both NBOHCs and their relative concentration does not change in agreement with previous results.[9,10]

Comparing our results with those of Sheng *et al.*,[9,10] we observe quantitative differences. We have found here a slow first-order kinetic with a decay time of the order of months, while Sheng *et al.*[9] reported a slow first-order kinetic of the order of a year (strongly dependent on the irradiation dose). A possible explanation for the differences with our experiments could be that Sheng *et al.* used 50 keV X-rays, while our experiments were carried out with beams of about 12 keV. However, the optical absorption spectra profiles are very similar in both cases, pointing out that the types of generated defects are the same despite the different X-ray

TABLE II. Parameters corresponding to the exponential fitting for the defects formation (left) and fading (right) kinetics switching on and off X-rays, respectively, at three different energies (11.80 keV, 11.92 keV and 11.95 keV).

Defects formation				Defects recuperation			
E (keV)	11.80	11.92	11.95	E (keV)	11.80	11.92	11.95
I_o	−2720	−1922	−3036	I_o	43	143	180
a	0.31	0.35	0.25	a	−0.01	−0.01	−0.02
γ_1(s)	2729	3245	3195	γ_1(s)	1053	877	1192
τ_1(s)	1891	2249	2215	τ_1(s)	730	608	826
b	2721	1922	3037	b	−43	−142	−180
γ_2(s)	1.93×10^8	1.72×10^8	2.34×10^8	γ_2(s)	6.94×10^6	2.95×10^7	4.12×10^7
τ_2(s)	1.34×10^8	1.19×10^8	1.62×10^8	τ_2(s)	4.81×10^6	2.04×10^7	2.86×10^7
R^2	0.9999	0.9996	0.9999	R^2	0.9994	0.9987	0.9991

energy. Our *in situ* fading measurements extended for a maximum of 6 h. With this recording time, it is difficult to measure precisely decay times of the order of months. Consequently, the slow kinetics data from Sheng *et al*. seem more reliable than ours. The main innovation of our experiments is the observation of a fast fading component of the order of ~10 min (see Table II), not previously reported. This component can be detected only by measuring the optical properties in real time at the irradiation site.

CONCLUSIONS

We have studied the effect of hard X-ray (11.9 keV) irradiation of soda-lime glasses on their optical properties. For this purpose, we have utilized a recently developed experimental setup, capable of simultaneously measuring XAS and SPR at a synchrotron beamline. The excitation of surface plasmons in a Au thin film grown on the glass is the probe used to monitor the induced optical changes in the glasses. We have identified two types of defects associated with the observed darkening: HC1 and HC2 centers. Monitoring, in real time, both the real and imaginary parts of the refractive index of the glass, we have determined two different dynamics by recombination with electrons in both the formation and fading of the induced defects. Together with a slow process with a characteristic time of the order of months, we have also identified a fast fading component with a much shorter characteristic time, of the order of minutes and not previously reported.

ACKNOWLEDGMENTS

This work has been supported by the Spanish Ministerio de Ciencia e Innovación (MICINN) through Project Nos. FIS-2008-06249 and MAT2009-14578-C03-02 and by Comunidad de Madrid, Project NANOBIOMAGNET (S2009/MAT-1726). A. Serrano thanks the CSIC for JAE-Predoctoral fellowship. We acknowledge the European Synchrotron Radiation Facility for provision of synchrotron radiation facilities and the Spanish Ministerio de Economía y Competitividad (MECC) and Consejo Superior de Investigaciones Científicas (CSIC) for financial support (PE-2010 6 0E 013) and for provision of synchrotron radiation facilities. We would like to thank the BM25-SpLine staff for the technical support and help far beyond their duties. Finally, the authors acknowledge C. de Julián Fernández for the access to the spectrophotometer at the Dipartimento di Chimica, University of Firenze. We would like to thank the referee for valuable comments and suggestions.

[1]A. Serrano, O. Rodríguez de la Fuente, V. Collado, J. Rubio-Zuazo, C. Monton, G. R. Castro, and M. A. García, Rev. Sci. Instrum. **83**, 083101 (2012).
[2]E. J. Friebele, *Radiation Effects in Optical and Properties of Glass* (Westerville, New York, 1991).
[3]*Defects in SiO_2 and Related Dielectrics: Science and Technology*, edited by G. Pacchioni, L. Skuja, and D. L. Griscom (Kluwer Academic, USA, 2000).
[4]*Structure and Imperfections in Amorphous and Crystalline Silicon Dioxide*, edited by R. A. B. Devine, J.-P. Duraud, and E. Dooryhe (Wiley, UK, 2000).
[5]*Silicon-Based Materials and Devices*, edited by H. S. Nalwa (Academic, USA, 2001).
[6]M. Rajaram and J. Friebele, J. Non-Cryst. Solids **108**, 1–17 (1989).
[7]C. E. Nurnberger and R. Livingston, J. Phys. Chem. **41**, 691 (1937).
[8]D. L. Griscom, J. Ceram. Soc. Jpn. **99**, 923 (1991).
[9]J. Sheng, K. Kadono, and T. Yazawa, Appl. Radiat. Isot. **57**, 813 (2002).
[10]J. Sheng, X. Yang, W. Dong, and J. Zhang, Int. J. Hydrogen Energy **34**, 3988 (2009).
[11]J. Sheng, K. Kadono, Y. Utagawa, and T. Yazawa, Appl. Radiat. Isot. **56**, 621 (2002).
[12]K. Kadono, N. Itakura, T. Akai, M. Yamashita, and T. Yazawa, Nucl. Instrum. Methods Phys. Res. B **267**, 2411 (2009).
[13]A. Kameyama, A. Yokotani, and K. Kurosawa, J. Appl. Phys. **95**, 4000 (2004).
[14]Nguyen Hong Ky, H. G. Limberger, R. P. Salathé, F. Cochet, and L. Dong, Opt. Commun. **225**, 313 (2003).
[15]H. Raether, *Surface Plasmons on Smooth and Rouge Surfaces and on Gratings* (Springer-Verlag, 1988).
[16]G. R. Castro, J. Synchrotron Radiat. **5**, 657 (1998).
[17]We simulated the spectra with the WINSPALL freeware code, see http://www.mpip-mainz.mpg.de/knoll/soft/ for WINSPALL freeware code.
[18]L. Dong, J. L. Archambault, L. Reekie, P. St. J. Russell, and D. N. Payne, Appl. Opt. **34**, 3436 (1995).
[19]N. Saliba, D. H. Parker, and B. E. Koel, Surf. Sci. **410**, 270 (1998).
[20]A. Bishay, J. Non-Cryst. Solids **3**, 54 (1970).
[21]L. Skuja, M. Hirano, H. Hosono, and K. Kajihara, Phys. Stat. Solidi (c). **2**, 15 (2005).
[22]J. W. H. Schreurs, J. Chem. Phys. **47**, 818 (1967).
[23]D. L. Griscom, J. Non-Cryst. Solids **64**, 229 (1984).
[24]J. Qui, X. Jiang, C. Zhu, M. Shirai, J. Si, N. Jiang, and K. Hirao, Angew. Chem., Int. Ed. **43**, 2230 (2004).
[25]Y. Bensimon, B. Deroide, F. Dijoux, and M. Martineau, J. Phys. Chem. Solids **61**, 1623 (2000).
[26]J. Sheng, J. Zhang, and L. Qiao, J. Non-Cryst. Solids **352**, 2914 (2006).
[27]Y. Samoilenko, Yu. Kaganovskii, A. A. Lipovskii, E. Mogilko, and M. Rosenbluh, Opt. Mater. **30**, 1715 (2008).